Nuclear Instruments and Methods in Physics Research A327 (1993) 87–91
North-Holland

NUCLEAR
INSTRUMENTS
& METHODS
IN PHYSICS
RESEARCH
Section A

Self-trapping kinetics of electrons in liquid neon

Werner F. Schmidt
Hahn-Meitner-Institute, Berlin, Germany

Yosuke Sakai
Hokkaido University, Sapporo, Japan

Alexei G. Khrapak
Institute for High Temperatures, Moscow, Russian Federation

After thermalization, an electron injected in a dielectric liquid is scattered by phonons and microscopical bubbles or holes. In the case of resonant scattering during its life time inside the bubble an electron can transfer its excess kinetic energy to the bubble walls and become localized. The proposed model explains qualitatively the strong dependence of the time of electron self-trapping on electric field strength and temperature found in liquid neon.

The photoelectrons are injected with an excess energy of several tenths of one eV into the conduction band of the liquid neon. They exhibit a high mobility and their state can be described by a delocalized wave functions. Due to elastic collisions with the neon atoms they will loose energy eventually reaching the bottom of the conduction band. Atomic density fluctuations give rise to fluctuations of the potential acting on the electrons. These fluctuations may lead to a temporary localization of the electrons in virtual or resonant states facilitating the formation of a deeper potential well. Finally, the formation of electron bubbles takes place. The electron wave function becomes localized. In this state the electron mobility is low and comparable to that of a negative ion. In this work we discuss the kinetics of the electron transition from the extended state to the electron bubble state.

The injection of excess electrons into the liquid is based on the photoelectric effect. A metal cathode immersed in the liquid is illuminated by a short flash of light of sufficiently short wave length. If the duration of the flash t_p is much shorter than the transit time of the electrons to the anode, t_d then we are dealing essentially with a thin layer of electrons moving in the electric field between cathode and anode. The current is given as,

$$i_{el}(t) = 0, \qquad t < 0; \tag{1a}$$

$$i_{el}(t) = eN/t_d, \quad 0 < t < t_d; \tag{1b}$$

$$i_{el}(t) = 0, \qquad t > t_d. \tag{1c}$$

where N denotes the total number of electrons in the layer, e is the electronic charge. The flash occurs at $t = 0$. During the duration of the flash, the current rises with a time constant, t_c determined by the electronic circuit for the measurement of the current. The same reasoning holds for the decay in time of the current when the electron layer reaches the anode. Here, in addition diffusion broadening of the layer during the transit leads to a somewhat larger decay time. Experimentally, one tries to work under the condition that $t_c < t_p$.

If electrons are trapped by impurities or density fluctuations of the liquid during their drift to the anode they are removed from the electronic current signal and decay of the signal in time results which is given by

$$i_{el}(t) = (eN/t_d)\exp(-t/t_1), \quad 0 < t < t_d. \tag{2}$$

Here, t_1 denotes the lifetime of the electrons with respect to the localization. For $t_1 < t_d$ the rectangular shape of the current signal (see eqs (1a)–(1c)) is replaced by an exponential decay of the roof but a sharp drop of the current at $t = t_d$ still remains. For $t_1 \ll t_d$ the exponential decay dominates and at a given sensitivity of the measuring circuit no discontinuity of the current is observed at $t = t_d$.

Examples of electron injection currents in liquid argon (for test), liquid and solid neon are shown in fig. 1. A perfectly rectangular trace was observed in liquid argon (see fig. 1a) indicating the absence of electron attaching impurities. In the ms time domain, the electron injection current in liquid neon exhibited the rectangular shape described by eq. (1) (see fig. 1b).

Superimposed was an oscillation due to the mechanical vibration of the electrodes excited by the laser pulse. The frequency of these oscillation was correlated with the mass of the electrodes. At much shorter times a fast electron current signal was observed which showed a decay in time described by eq. (2) (see fig. 1c). With increasing applied field strengths this signal approached more and more the rectangular shape of eq. (1) (see fig. 1d). The signal obtained in solid neon at short times corresponded to the shape described by eq. (1) (see fig. 1e). The oscillations superimposed on the fast signals are due to the imperfect matching of the cell to the wave impedance of the measurement circuit. From such traces, drift times t_d and decay times t_1 as a function of electric field strength and temperature were obtained. At higher temperatures, the decay time

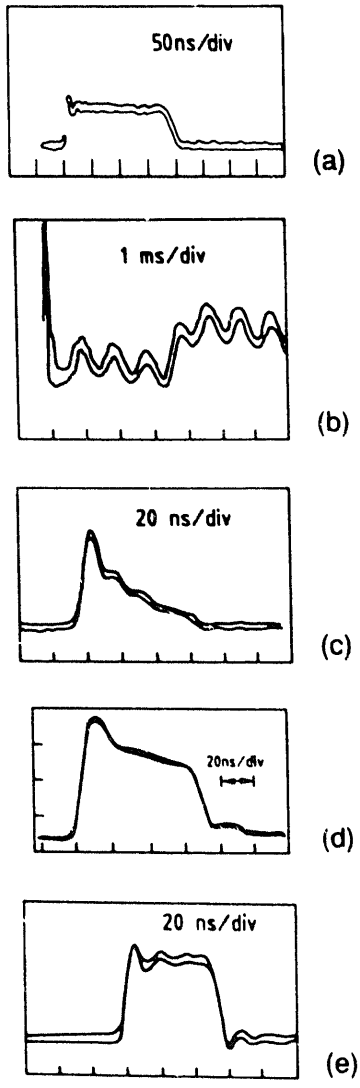

Fig. 1. Oscilloscopic traces of electron injection currents; (a) LAr at $T = 87$ K, (b) LNe at $T = 25.85$ K, $E = 14.3$ kV/cm; (c) LNe at T = 25.85 K, $E = 52.9$ kV/cm; (d) LNe at $T = 25$ K, $E = 97.1$ kV/cm; (e) SNe at $T = 20$ K, $E = 8.75$ kV/cm.

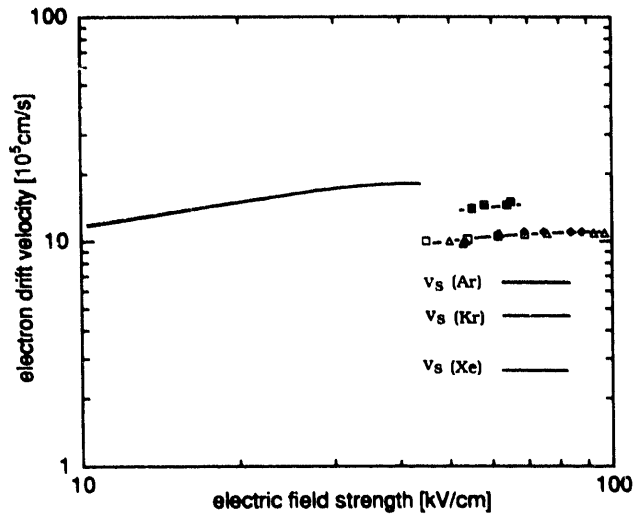

Fig. 2. Fast electron drift velocity in neon; ——— solid neon [13]; ■ LNe and H_2 at 25K; △ LNe at 25 K, vapor pressure; □ LNe at 25 K, pressurized by neon gas to 18 bar; ◆ LNe at 26 K, pressurized by neon gas to 27 bar.

t_1 decreased to such an extent that determination of a drift time by a discontinuity of the electron current signal was no possible anymore. Under these conditions, a relative measure of the electron drift time was obtained by measuring the initial amplitude of the electron current signal. According to eq. (2), the initial current amplitude is inversely proportional to t_d (see eq. (2) for $t = 0$).

Evaluation of the fast electron current signals according to eq. (2) gave drift times, t_d and lifetimes, t_1. The fast electron drift velocities obtained as a function of electric field strength are shown in fig. 2. The data could be obtained over limited field strength range only. At lower value of the field strength t_1 became short compared to t_d so that no knick points were visible in the signal traces. At electric field strengths exceeding 50 kV/cm saturation of the drift velocity occurred. At 25 K, a value of $v_s = 1.1 \times 10^6$ cm/s was obtained. The fast electron drift velocities in liquid neon have the same value as in liquid argon, krypton, xenon [1] and in solid neon [2] where electrons can exist only in extended state. The exponentially decaying part of the signal yielded the life time of the fast electron. It depends on the applied electric field strength. The data obtained are shown in fig. 3. Increase of the temperature at a given field strength led to a decrease of the electron lifetime.

The life time t_1, of an electron in the extended state with respect to capture and localization can be written as

$$t_1^{-1} = \langle N_c \sigma_c v \rangle, \tag{3}$$

where N_c is the concentration of traps, σ_c is the cross section for capture and v is the velocity of the electron.

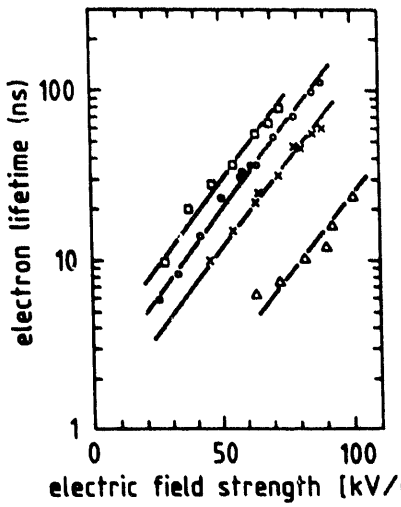

Fig. 3. Lifetime of the fast electrons in LNe as a function of the electric field strength; parameter-absolute temperature: □ 24.9 K, ○ 25 K, × 26.8 K, △ 30 K.

The brackets $\langle \cdots \rangle$ signify the averaging over the electron velocities, and over the sizes and magnitudes of the fluctuations. The experimentally found strong dependence of t_1 on the field strength E and on the temperature T is determined by the dependence of the electron velocity distribution function $f(v)$ on E and T, and by a possible dependence of N_c on T.

In solid neon, thermalized delocalized electrons move at the bottom of the conduction band. The energetic position of this level is usually designated as V_0 which is approximately +1 eV in solid neon. Melting leads to a strong increase of the concentration of defects which in turn lowers the value of V_0 to +0.67 eV [3]. This value reflects an overall homogenous distribution of single atom vacancies, which we also called bubblons in liquids [4]. In addition, fluctuations of the concentration of the defects exist in the liquid. These fluctuations are correlated with fluctuations of the potential. In the case $V_0 > 0$, a higher concentration of single atom vacancies or bubblons in a given volume will lead to a slight depression of the potential, or in other words, V_0 would be smaller in this regions as compared to the bulk. A smaller concentration of vacancies in a given region would lead to an increase of V_0. These fluctuations are relatively extended and cannot lead to temporary localization due to their shallow nature. Fluctuations consisting of one or several atomic vacancies represent deep potential wells with potential walls at which the electron is scattered. Virtual or resonant electronic energy levels may appear in the potential wells. Between the potential walls the electron is reflected many times, making its residence time much longer than the classical time required for passing the fluctuation. During its residence at the fluctuation, the electron is losing energy due to elastic collisions with the potential walls. Capture of the electron is possible if during the time of residence t_f at the fluctuation the electron loses its excess kinetic energy. The cross section for capture σ_c can therefore be written as,

$$\sigma_c = \sigma_{el} P_c \approx \sigma_f \theta(t_f - t_k), \tag{4}$$

where σ_f is the cross section for elastic electron scattering on the fluctuation, P_c is the probability of electron capture, t_k is the time necessary to transfer the kinetic energy of the electron to the walls of the fluctuation, θ-function is defined as $\theta(x) = \{0, x < 0; 1, x > 0\}$. The scattering cross section of an electron on a fluctuation with resonant properties is well known [5]

$$\sigma_f = 4\pi/(k^2 + k_1^2), \tag{5}$$

where $k = 2\pi mv/h$ is the electron wave number (m is the electron mass, h is Planck's constant). The value of k_1 is related to the energy of the resonant state, $E_1 < 0$, or of the virtual state, $E_1 > 0$, by the following expression,

$$k_1^2 = 8\pi^2 h^{-2} m |E_1|. \tag{6}$$

In the further discussion, for simplicity, we will consider as fluctuations empty voids of spherical shape, only. For almost resonant voids of radius R, $|E_1| \ll |V_0|$ and E_1 is given as,

$$|E_1| \approx 2\pi^2 h^{-2} mR^2 \left[V_0 - h^2/(32mR^2)\right]^2. \tag{7}$$

From eqs. (5)–(7), it is obvious that the cross section for capture σ_c, exhibits a sharp maximum for $E_1 = 0$ or when,

$$R^2 = R_0^2 = h^2/(32mV_0). \tag{8}$$

The time of residence t_f, at the void is also well known [6],

$$t_f = (2R/v)2k^2/(k^2 + k_1^2) = 2mh^{-1}kR\sigma_f. \tag{9}$$

This time also exhibits a maximum for $R = R_0$, when $k_1 = 0$. In the case of low energy electrons, their velocity v, is small, and the time of residence at the void,

$$t_f(R_0) = 4R_0/v \tag{10}$$

is many times the classical time t_{cl}, requires for passing the void,

$$t_{cl} = 2R_0(m/2V_0)^{1/2} = 8mh^{-1}R_0^2. \tag{11}$$

For an estimation of the time necessary for the electron to lose its kinetic energy at the void and become captured, we note that qualitatively two different processes occur: The first process consists of the a fast transition of the electron to the virtual or resonant energy level; this process is practically not accompanied by any changes in position of the atoms surround-

ing the void. The second process is a slow adiabatic motion of the occupied resonant level due to the electron pressure coupled with expansion of the void leading eventually to the formation of a microscopic bubble containing the electron. The effective mass of the wall of the spherical void is very large in comparison with the electron mass. As a consequence, during the residence time t_f of the electron the energy level E_1 changes very slowly. The pressure p_e, exerted by the electron on the walls is given as [5],

$$p_e = h^2/(16\pi m R^5). \tag{12}$$

The effective mass M_R, for the radial movement of the walls of the spherical void in an ideal incompressible liquid is given as,

$$M_R = 3M, \quad M = (4\pi/3)R^3 d, \tag{13}$$

where M is the mass of the liquid displaced by the void; d is the density of liquid. The equation of motion of the wall can then be written as,

$$M_R \frac{d^2R}{dt^2} = 4\pi R^2 p_e = h^2/(4mR^3). \tag{14}$$

Integration of eq. (14) is carried out by taking into account that at $t = 0$, the electron energy is equal to $mv^2/2$ while at $t = t_k$ it is zero, We obtain for t_k,

$$t_k = (2/\pi h)(M_R m)^{1/2} R_0^3 k. \tag{15}$$

The condition $t_f > t_k$, expressed in eq. (4) restricts the energy of electrons capable of being captured to

$$E(k) = h^2k^2/(8\pi^2 m) \le h^2/\left[2(M_R m)^{1/2} R_0^2\right] = E(k_r). \tag{16}$$

In neon, $R_0 = 3.8 \times 10^{-8}$ cm and $M_R/m \approx 10^5$; it follows that only electrons with an energy smaller $E(k_r) = 11$ meV or $T_e = 130$ K can undergo autolocalization. In the range of electric field strength where we studied experimentally the lifetime t_1, the mean electron energy is of the order to one eV. Therefore, only a small part of the electron collective can be localized at preexisting spherical voids.

The distribution function $n_c(R)$ of spherical voids of radius R for the conditions of the saturation curve is given by,

$$n_c = B \exp\{-4\pi\sigma R^2/k_B T\}. \tag{17}$$

The constant B can be estimated from the fact that at triple point, voids occupy approximately 15% of the liquid volume, i.e.

$$(4\pi/3)\int_0^\infty R^3 n_c(R)\, dR \approx 0.15. \tag{18}$$

Introducing eq. (17) into eq. (18) yields,

$$B = (0.45/2\pi)(4\pi\sigma/k_B T)^2 \exp(y_s)/(y_s - 1), \tag{19}$$

with

$$y_s = 4\pi\sigma r_s^2/k_B T, \quad r_s = (3/4\pi N)^{1/3}, \tag{20}$$

where r_s is the radius of the elementary cell of the liquid, N is the number density of the liquid. For the process of localization, the spherical voids with radii $R = R_0 \pm R'$ are important whereby R' is of the order of 1 atomic radius. For the estimation we consider the concentration N_R of voids with $R \ge R_0$ given as,

$$N_{R>R_0} = \int_{R_0}^\infty n_c(R)\, dR, \tag{21}$$

which yields taking into account eqs. (17), (19) and (20),

$$N_{R>R_0} = Bk_B T/(8\pi\sigma R_0) \exp(-y_0),$$
$$y_0 = 4\pi\sigma R_0^2/k_B T. \tag{22}$$

Inserting parameters for neon into eq. (22) yields $N_{R>R_0} = 1.4 \times 10^{12}$ voids/cm^3. The number of electrons injected in our experiments is of the order of 10^8 per laser pulse.

Eq. (3) can now be rewritten and the life time t_1 is obtained as,

$$t_1^{-1} = n_c(R_0)4\pi(h/2\pi m)^4 \cdot \int_0^\infty k^3\theta(k - k_r) f(hk/2\pi m)\, dk \times 4\pi\int_0^\infty \left[k^2 + (\pi^2/16)(R - R_0)^2/R_0^4\right]^{-1} dR. \tag{23}$$

For the electron energy distribution function we assume

$$f(v) = A \exp(-\alpha v^2 - \beta v^4). \tag{24}$$

The term βv^4 describes a Druyvesteyn type distribution. Druyvesteyn is used to describe the energy distribution of electrons in gases at moderately high values of the electric field strength. The term αv^2 describes the energy distribution at very high electric fields, where the electron drift velocity saturates [7]. Unfortunately, eqs. (22) and (24) cannot be used at low electric field strengths where v_d is proportional to E. If we introduce eq. (24) into eq. (23), we obtained,

$$t_1^{-1} \approx (64/3)\pi^2(h/2\pi m)^3 A n_c(R_0) R_0^2 k_r^3. \tag{25}$$

The dependence of t_1 on the electric field strength is contained in the constant A. In the case of moderately strong electric field strength, experimentally the drift velocity v_d was found to be proportional to $E^{1/2}$ in LAr, LKr and LXe. At higher values of the electric field strength, v_d is increasing as E^x with $x < 0.5$ eventually reaching saturation at high fields ($\gg 50$ kV/cm). Similar dependencies can be also inferred from our measurements for LNe (see fig. 2). For $x =$

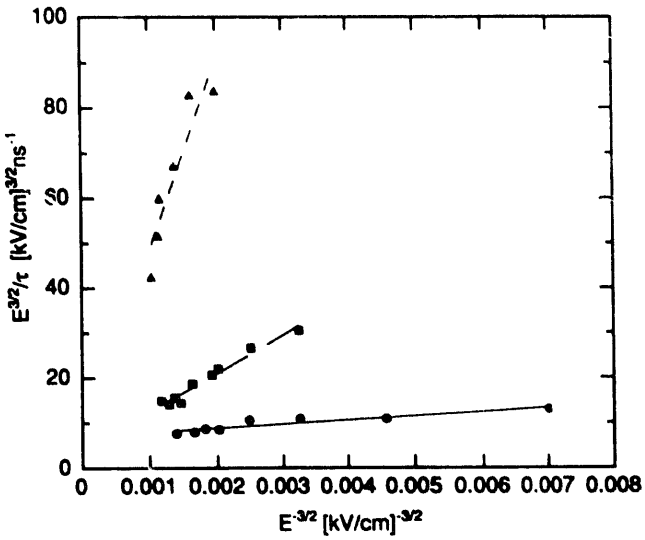

Fig. 4. Dependence of electron life time in the delocalized state as a function of electric field strength; comparison between experimental data (fig. 3) and predictions of eq. 26; ▲ 30 K, ■ 26.8 K, ● 24.9 K.

0.5, A is proportional to $E^{-3/2}$ while for $x = 0$, A is proportional to E^{-3}. After interpolation, eq. (25) can be written as,

$$t_1^{-1} \approx C_1 E^{-3/2} + C_2 E^{-3} \quad \text{or} \quad t_1 E^{3/2} \approx C_1 + C_2 E^{-3/2}. \tag{26}$$

A plot of the data of fig. 3 according to the last equation is shown in fig. 4. Reasonably good agreement is observed which might serve as an indication of the fidelity of our model.

References

[1] W.E. Spear and P.G. LeGomber, in: Rare Gas Solids, Vol. 2, eds. M.L. Klein and J.A. Venables (Academic Press, New York, 1977) p. 1119.
[2] Y. Sakai, E.H. Böttcher and W.F. Schmidt, Z. Naturforsch. A37 (1982) 87.
[3] W. Tauchert, H. Jungblut and W.F. Schmidt, Can. J. Chem. 55 (1977) 1860.
[4] A.G. Khrapak, Soviet Phys. - JETP Lett. 47 (1988) 445.
[5] L.D. Landau and E.M. Lifshitz, Quantum Mechanics, Nonrelativistic Theory (Pergamon, Oxford, 1965).
[6] A.I. Baz', Y.B. Zeldovich and A.M. Perelomov, Scattering, Reactions and Decays in Non-relativistic Quantum Mechanics (Nauka, Moscow, 1971), in Russian.
[7] B.M. Smirnov, Physics of Weakly Ionized Gases (Nauka, Moscow, 1977) in Russian.